

The Indian Journal of Radiology & Imaging

Indian J Radiol Imaging. 24(2): 139-148

Imaging and intervention in prostate cancer: Current perspectives and future trends

Sanjay Sharma

Department of Radiodiagnosis, All Institute of Medical Sciences, New Delhi, India

Correspondence: Dr. Sanjay Sharma, Department of Radiodiagnosis, All Institute of Medical Sciences, New Delhi - 110 029, India. E-mail: drssharma@hotmail.com

Copyright: © Indian Journal of Radiology and Imaging

DOI: 10.4103/0971-3026.134399

Published in print: Apr-Jun2014

Abstract

Prostate cancer is the commonest malignancy in men that causes significant morbidity and mortality worldwide. Screening by digital rectal examination (DRE) and serum prostate-specific antigen (PSA) is used despite its limitations. Gray-scale transrectal ultrasound (TRUS), used to guide multiple random prostatic biopsies, misses up to 20% cancers and frequently underestimates the grade of malignancy. Increasing the number of biopsy cores marginally increases the yield. Evolving techniques of real-time ultrasound elastography (RTE) and contrast-enhanced ultrasound (CEUS) are being investigated to better detect and improve the yield by allowing “targeted” biopsies. Last decade has witnessed rapid developments in magnetic resonance imaging (MRI) for improved management of prostate cancer. In addition to the anatomical information, it is capable of providing functional information through diffusion-weighted imaging (DWI), magnetic resonance spectroscopy (MRS), and dynamic contrast-enhanced (DCE) MRI. Multi-parametric MRI has the potential to exclude a significant cancer in majority of cases. Inclusion of MRI before prostatic biopsy can reduce the invasiveness of the procedure by limiting the number of cores needed to make a diagnosis and support watchful waiting in others. It is made possible by targeted biopsies as opposed to random. With the availability of minimally invasive therapeutic modalities like high-intensity focused ultrasound (HIFU) and interstitial laser therapy, detecting early cancer is even more relevant today. [^{18}F]-fluorodeoxyglucose positron emission tomography/computed tomography (^{18}F FDG PET/CT) has no role in the initial evaluation of prostate cancer. Choline PET

has been recently found to be more useful. Fluoride-PET has a higher sensitivity and resolution than a conventional radionuclide bone scan in detecting skeletal metastases.

Introduction

Prostate cancer is a major public health problem worldwide. It is the commonest visceral malignancy in men and the second leading cause of cancer death in the Western world after lung cancer. In India, its incidence is stated to be lower than in the Western countries. The latest population-based cancer registry in India by Indian Council of Medical Research (ICMR) records the age-adjusted rate (AAR) to be 8.4, 10.7, 7.7, and 1.9 per 100,000 population in the cities of Bangalore, Delhi, Mumbai, and rural Barshi, respectively.[1] Prostate cancer is among the five leading cancers in the Indian metro cities. With the growing aging population, the incidence of prostate cancer is expected to increase further in some countries. The year 2014 is expected to see an addition of estimated 233,000 new cases in the United States alone.[2] Japan, with its second highest life expectancy at 78.6 years, has shown a sharp increase in its incidence, ahead of even the cancers of stomach and lung.[3]

Autopsy evidence suggests that a third of men over 50 years and 80% men above 80 years of age show histological foci of prostate cancer.[45] It is surprisingly high, and almost an age-related phenomenon. However, its malignant potential varies widely from asymptomatic to rapidly progressive systemic disease at presentation. Many of these cancers may remain clinically occult and never manifest in patients' life time. Most patients, therefore, die with rather than of the disease. One of the major challenges in prostate cancer evaluation is to differentiate indolent cancers from those which are clinically relevant.

Prostate Cancer Screening

All men aged 60 years or older presenting with lower urinary tract symptoms are now offered serum prostate-specific antigen (PSA) testing. The diagnostic evaluation in prostate cancer is initiated by elevated serum PSA levels and abnormal Digital Rectal Examination (DRE). However, a definitive diagnosis is currently established only by the subsequent transrectal ultrasound-guided biopsy (TRUS biopsy). The tissue is subjected to histopathologic analysis for determining the cancer grade (Gleason score) and volume.[6] The prognosis and choice of therapy is dependent on this information.

The DRE assesses the shape, size, symmetry, consistency, and nodularity of the gland and helps in assessing the clinical stage of prostate cancer. However, its overall sensitivity is low at 37% in the serum PSA range 0-3 ng/ml.[7] DRE is not considered accurate for detecting and staging prostate cancer.[8] Serum PSA-based cancer diagnosis has higher detection rates than DRE. It has a low overall specificity of 36%.[9] Serum PSA is “prostate specific” and “not cancer specific,” and is falsely elevated in benign prostatic hyperplasia (BPH), prostatitis, trauma, and urinary retention. Serum PSA estimation and DRE together possess a low sensitivity and specificity, with up to 25% prostate cancer patients showing a normal PSA and over 50% having normal DRE.[10] Despite this, it remains perhaps the best test for early detection of prostate cancer. Increasing number of cancers are being detected at an early stage when they are smaller and more treatable.[11] Indisputably, the determination of serum PSA has had a massive impact on prostate cancer management.

Is there a “Cut-Off” Serum PSA Level to Detect Prostate Cancer?

A cut-off level for serum PSA is age-dependent. A level above 2.5 ng/ml in patients younger than 60 years and above 4 ng/ml at any age warrants a prostate biopsy.[12] The PSA velocity of >0.75 ng/ml/year regardless of an absolute PSA level is also considered significant.[12] The PSA density of <0.15 ng/ml/cc suggests BPH, free/total PSA ratio <10 suggests cancer, and a ratio >25 suggests BPH.[13] The latter tests are not routinely employed in clinical practice.

Serum PSA for Screening Prostate Cancer: Impact on Survival

PSA-based screening results in significant increase in prostate cancer detection rate at an early and potentially more treatable stage. It is predicted that PSA-based screening can help to reduce the mortality by 20%, but at a high cost of overdiagnosis and overtreatment.[14] To avoid overdetection of prostate cancer, the European Guidelines Committee (EGC) does not recommend routine serum PSA testing in patients younger than 50 years or those having a life expectancy less than 10 years. Prostate Cancer Gene 3 (PCA) is a new biomarker that has been recently discovered. It is highly specific for cancer and is not influenced by prostatitis. However, it is currently too expensive for routine clinical use.[15]

TRUS-Guided Systematic Biopsy

The TRUS-guided biopsy (TRUSgBx) is random, but has advantages of its ease of use and real-

time capability. Despite its shortcomings, it continues to remain the standard of care. The sextant prostatic biopsy has a sensitivity of 60%, positive predictive value of 25%,[\[1617\]](#) negative predictive value of 70-80%,[\[9\]](#) and false-negative rate between 10 and 38%.[\[18\]](#) Up to 35% cancers are missed on first biopsy.[\[19\]](#) Gleason grade is underestimated in 46%.[\[20\]](#) Accuracy further decreases with increasing gland size. The issue of missed cancers could be addressed by obtaining multiple biopsies or alternatively by repeating sextant biopsies. Image-guided “targeted” biopsy specifically obtained from the suspicious foci could be yet another approach, but TRUS is blind to 40% cancers which appear isoechoic.[\[21\]](#)

Prostate Biopsy Schemes

Sextant biopsy scheme is now considered inadequate, and has given way to the extended core biopsy protocols consisting of obtaining 10, 12, or more (saturation biopsy) cores. Presti et al.[\[22\]](#) demonstrated an increased diagnostic yield to 33.5%, 39.7%, and 40.2% as the number of cores was increased from 6 to 8 to 10, respectively. Similarly, Babian et al.[\[23\]](#) showed an increased diagnostic yield from 20% to 30%, as the cores were increased from 6 to 11, respectively.

Grade of Malignancy: Gleason Score

Prostate cancer is typically multi-centric and heterogenous. Foci of cancers located in different regions of gland in the same patient tend to have different grades of malignancy.[\[24\]](#) Two most abundant areas of malignancy in that order are histologically graded on a scale of 1-5 from most well differentiated (score 1) to least differentiated (anaplastic) (score 5), and the final score is presented as a combination (e.g. 3 + 5 or 4 + 3, etc.). Gleason score is the single strongest prognostic factor for clinical behaviour and treatment response in prostatic cancer.[\[6\]](#) Therefore, besides the accurate clinical staging, the cancer grading is necessary to plan the optimum choice of treatment.

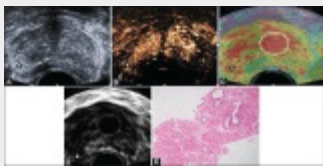
Need for Imaging

A combination of the above clinical tools (serum PSA + DRE + TRUSgBx) often results in an incorrect diagnosis and inaccurate risk assessment, leading to less optimal choice of therapy.[\[810131617181920\]](#) According to the general clinical perception, imaging is not for detection of prostate cancer. Until very recently, the imaging for prostate cancer has primarily been used firstly to stage a high-risk localized cancer that needs radical treatment and secondly to exclude

patients with advanced disease in whom hormonal treatment or external beam radiotherapy is the choice rather than surgery. Over half of the cancers at presentation in India are already locally advanced or metastatic, precluding curative surgery.[2526] Lately, there has been a paradigm change in the therapy of early localized prostate cancer due to the growing popularity of minimally invasive therapy by radiofrequency ablation (RFA) or LASER, making detection and localization of early cancer even more relevant. From the surgical standpoint, it is vital for a radiologist to differentiate a T2 (organ-confined) from T3 (extracapsular spread) disease. Patients with clinically localized disease (T1 and T2) have a low probability of metastatic disease. Most PSA diagnosed prostate cancers tend to be organ-confined.[11]

Transrectal USG

It is a widely available, low-cost tool used for morphological assessment of prostate gland. However, it can neither reliably diagnose an intra-prostatic cancer nor detect its extracapsular extension. Although most cancers in the peripheral zone (PZ) are hypoechoic, some are hyperechoic [Figure 1A]. Others, including central gland cancers, remain difficult to diagnose. Therefore, alone, it cannot be used for screening of prostate cancer. Its main current role, therefore, is to guide prostatic biopsies.



[View larger version](#)

Figure 1(A-E). A 76-year-old man with lower urinary tract symptoms, serum PSA 32.2 ng/ml. Gray scale TRUS (A), CEUS images (B), paired elastogram (colour C; gray scale D), and photomicrograph (E) (H and E) of TRUS guided biopsy; all showing an ill circumscribed nodule (star) in the PZ of mid-gland on the right corresponding to an area of abnormality on per-rectal examination. This nodule is hyperechoic (A), shows enhancement (B) and relatively hard (C, D). Hard areas are displayed as red and soft areas as green. On histopathology the nodule was diagnosed to be a cancer on histopathology. Three out of 12 cores showed features of high grade, Gleason score 10 (5+5), adenocarcinoma. Note the persistent enhancement of the central gland and another larger hard nodule (C, D; encircled) in the central gland on the left. This was a benign hyperplastic nodule on histopathology.

Ultrasound Color and Power Doppler Imaging

It has been suggested that color and power Doppler examinations may be helpful in detecting isoechoic tumors which are otherwise missed on gray-scale imaging.[2728] However, it is now well known that these techniques do not reliably identify all malignant foci, and thus cannot obviate the need for a systemic biopsy at the present time.[2930] Doppler USG is unable to identify the microscopic vessels of prostate cancer which are typically of the order of 10-15 μm in diameter and do not possess enough flow to cause Doppler shift. The flow detected is due to larger

feeding vessels.

To increase the sensitivity of TRUS and reduce the number of core biopsies, several new technologies in conjunction with standard TRUS have been investigated. Particularly promising are contrast-enhanced ultrasound (CEUS) and real-time elastography (RTE). CEUS is gradually gaining acceptance as a tool to improve cancer detection.

Contrast-Enhanced USG

Sonographic contrast media are stabilized micro-bubbles (1-10 μm) of gas in an encapsulated shell. Unlike radiographic contrast media which freely diffuse into tissue, most micro-bubbles are blood pool agents that remain confined to the vascular lumen, where they persist until they disintegrate. They have an excellent safety profile, though many of them are still not approved by the US Food and Drug Administration (FDA) or European agencies. These are used in conjunction with harmonic imaging and low-energy (mechanical index) echoes. Foci of cancer enhance with contrast due to increased vascularity [[Figure 1B](#)]. Studies have shown a significant increase in cancer detection rate using CEUS-targeted biopsies compared to random biopsies.[[3132](#)] Majority of these cancers detected are of high grade. Nonetheless, the ability of this technique to discriminate benign from malignant lesions is low and its application in guiding targeted biopsy needs to be validated in larger studies. A recent Italian study[[29](#)] in 300 subjects did not significantly improve the cancer detection rate with the use of color Doppler USG with or without USG contrast.

Real-Time Elastography

In recent years, substantial progress has been made in the field of ultrasound-based RTE that measures the tissue elasticity. The tenet of elastography is that the cancerous tissues possess a relatively increased stiffness as a result of increased cell density. In “strain imaging,” the images are obtained with and without manual compression of prostate, and the degree of displacement (strain) produced as a result is used to generate an elastogram (color maps) in real time. However, in the “shear wave technique,” the shear waves are produced which travel at a right angle to the insonating beam. These travel faster in the stiffer tissues and, therefore, provide a measure of tissue elasticity in quantitative terms. This technology is considered superior and more reproducible than strain imaging. The hard areas presumably representing cancer foci are shown as red areas in the color elastogram map [[Figure 1C](#)] and appear dark and larger than the

corresponding gray-scale image [Figure 1D]. A recent large prospective study showed a sensitivity of 68-86% and specificity of 72-81% using RTE in the diagnosis of organ-confined prostate cancer.[33] [TAG:2][TAG:2] It is, therefore, considered a promising adjunctive technique to the standard gray-scale TRUS to guide targeted prostatic biopsies. However, further improvement is currently required to justify its routine clinical use.

Our Study Using RTE and CEUS in the Diagnosis of Prostate Cancer

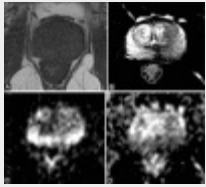
An ongoing (unpublished) prospective study at our institute recruited 34 suspected prostate cancer patients (mean age 66.3 years, mean PSA 24.4 ng/ml). Up to five targeted biopsies were performed from the suspicious areas, i.e., hard on RTE and/or enhancing on CEUS, followed by standard 12-core random prostatic biopsy. Analysis of the cancer detection rate using random and targeted biopsies was made both “by core” and “by patient.” In the former, the random TRUSgBx resulted in the detection rate of 31.9% cores compared to 42.8% ($P = 0.06$), 61.9% ($P < 0.05$), and 12.4% ($P < 0.05$) cores using RTE, CEUS, and RTE + CEUS, respectively. However, in the latter, the random TRUSgBx resulted in detecting 88.9% patients, compared to 83.3% and 72.2% patients using RTE and CEUS, respectively. These preliminary results suggest that RTE and CEUS do have a potential to reduce the number of cores, thereby making the biopsy procedure less invasive, but do not help to diagnose additional patients.

USG technology has also been studied in few other ways. Computer-aided diagnosis (CAD) using TRUS reduces inter-operator variability and compensates for low sensitivity and specificity of human eye interpretation. However, the inherently low resolution of TRUS remains its main limitation. Ultrasound spectroscopy uses RF echo signals to discriminate benign from malignant tissues. 3D TRUS provides excellent anatomical reference points. The potential of these newer USG-based techniques is yet to be validated by further studies.[3435]

Magnetic Resonance Imaging

Since the first prostate magnetic resonance imaging (MRI) done in mid 1980s, it has established itself as a main diagnostic modality. Currently, it provides not just anatomical (T1 and T2WI) but also functional information, through diffusion-weighted imaging (DWI), magnetic resonance spectroscopy (MRS), and dynamic contrast-enhanced imaging (DCE). In multi-parametric imaging, the anatomical and functional information is integrated. Currently, MRI finds its clinical applications in all aspects of prostate cancer evaluation.

Conventional T2W MR images display prostatic zonal anatomy at a high spatial resolution. Nearly 80% cancers arise in the PZ and are seen as low signal focus within the normal bright PZ [Figure 2B]; however, prostatitis, hyperplastic nodules, infarction, scars, hemorrhage, and calcification may mimic these appearances.[3637] Cancers arising from the transitional zone (TZ) are generally indistinguishable from the surrounding gland owing to the heterogenous signal of the hyperplastic central gland on T2W images.[3637] MRI signal depends upon the Gleason score, cellular density, and cancer growth pattern. However, the focal low signal areas within the PZ may not always represent cancers. Also, there is overlap in appearance with BPH in the central gland. With aging, BPH in the TZ compresses the central zone (CZ) into a thin rim of pseudo-capsule.



[View larger version](#)

Figure 2(A-D). A 77-year-old man reported with serum PSA 11.6 ng/ml. MR images at the mid-gland, T1WI (A), T2WI (B), DWI (C), and ADC map (D). The intermediate signal intensity gland is seen on T1WI; T2WI shows ill-defined hypointense area posteriorly at the PZ, especially prominent on the left. There is no extracapsular extension or regional adenopathy. The entire PZ on the DWI shows restricted diffusion as evidenced by bright signal on DWI and dark signal on ADC maps. On TRUS-guided biopsy, 4 out of 12 cores showed features of adenocarcinoma, Gleason score 9 (4 + 5)

Diffusion-weighted imaging

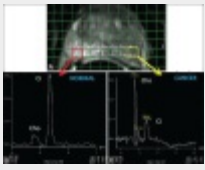
It provides information about the molecular environment of biological tissues by applying motion-encoding gradients which cause phase shifts in the moving protons. The “b value” determines the amount of diffusion weighting and apparent diffusion coefficient (ADC). The b values of up to a 1000 s/mm^2 are typically used for prostate cancer evaluation. Higher values may increase the accuracy of cancer detection, especially in the TZ.[3839] Rich glandular architecture of normal PZ allows extensive diffusion that accounts for higher ADC. In cancer, there is destruction of this glandular structure, with increased cell density and decreased interstitial volume leading to restriction of diffusion or lower ADC [Figures 2C and D]. At a strength of 1.5 T, without the use of endorectal coil (ERC), the mean ADC ($\times 10^3 \text{ mm}^2/\text{sec}$) for healthy PZ and cancer was found to be 1.72-1.85 and 0.96-1.02, respectively.[404142] However, with the use of ERC, the mean ADC for healthy PZ and cancer has been found to be 1.51-1.69 and 1.39, respectively.[424344] There is no single cut-off ADC value to predict cancer as it is dependent on many variables, including b value,[45] MR field strength,[46] the coil employed,[43] overlap between healthy tissue and cancer,[47] location of cancer within the gland (ADC: PZ > TZ),[48] and age (ADC in central gland increases with age),[40] among others.

Various studies and trials have now firmly established the incremental role of DWI over the

conventional anatomical MRI.[424950] The strength of DWI is that it is fast, simple, and readily available. It provides high contrast between cancer and normal tissue. The shortcomings are that it has poor spatial resolution (even at 3T) and is subject to motion artifacts and susceptibility-induced distortion. The latter is especially relevant as diffusion-weighted MR images are degraded as a result of local hemorrhage following prostatic biopsy. Current clinical use of DWI is for all indications of prostate cancer evaluation, which include detection, localization, characterization, biopsy guidance, and active surveillance. However, for cancer staging, it is not an ideal technique owing to its lower spatial resolution.[51] The correlation of DWI with histopathologic findings and prognostic factors remains an area of further research.

Magnetic resonance spectroscopy

It provides spatial information about the relative concentration of different intracellular metabolites in contiguous small voxels of prostatic tissue. It is performed in 3D, using commercially available software after suppressing the signal from water and fat. The multi-voxel MR spectroscopic data is overlaid on the T2W image to distinguish the normal prostatic tissue with abnormal voxels representing cancer [Figure 3A]. Various metabolites resonate at different frequencies within the spectrum, viz., choline resonates at 3.2 ppm, polyamine at 3.1 ppm, creatine at 3.0 ppm, and citrate at 2.6 ppm [Figure 3B]. Polyamine is an inconstant peak. Choline and creatine peaks cannot be separately resolved at 1.5 T. Classically, a ratio of $(\text{Cho} + \text{Cr})/\text{Cit}$ that is 2 SD above mean indicates possible cancer and 3 SD above mean is very suggestive of cancer [Figure 3C].[52] Higher ratios are increasingly more suggestive of cancer indicating its potential role in predicting the aggressiveness of prostate cancer. Addition of spectroscopy to MRI improves its ability to localize the disease more precisely, reducing inter-observer variability, but it is yet to become the standard of care. MRS is potentially more useful than MRI in detecting T2 cancers;[53] however, the cancer metabolite ratio here varies broadly, having an overlap between benign and malignant tissues. Significantly increased $(\text{Cho} + \text{Cr})/\text{Cit}$ ratio in larger tumors also suggests its potential in volume estimation.[54] Combined MRS and MRI have improved accuracy in determining extracapsular extension.[55]



[View larger version](#)

Figure 3(A-C). A 69-year-old man presented with serum PSA 21.4 ng/ml. Overlay of MR spectroscopic matrix and multi-voxel spectra on the T2W image of mid-prostate (A). The voxel on the left (yellow) shows markedly reduced citrate (Ci) signal and increased chol-creatine (Cho + Cr)-to-citrate ratio consistent with cancer (C). On TRUS-guided biopsy, this was later confirmed to be a high-grade cancer, Gleason score 9 (5 + 4). The voxel on the right (red) represents a normal spectrum (B). The addition of spectroscopy to MRI improves the ability to localize the cancer more precisely reducing the inter-observer variability. Higher the metabolite ratio, higher are the chances of finding a high-grade cancer

Advantages of MRS are that it is a robust and well-established technique with generally accepted accuracy and high specificity. It possesses a sufficiently high signal-to-noise ratio (SNR) even at 1.5 T, with a resolution of 0.4 cm^3 . Better spectral dispersion can be obtained by higher field strength. The shortcomings include its long imaging time. It is technically more challenging than all other functional MR techniques. Learning to interpret the MRS data requires time and experience. Spectral quality is reduced by the field inhomogeneity and susceptibility-induced distortion by hemorrhage. Therefore, a delay of approximately 8 weeks is recommended after the last prostatic biopsy. Currently, MRS is used in prostate cancer for all indications that include detection, localization, staging, characterization, biopsy guidance, and active surveillance. The automated measurement procedures and rapid display of results remain areas of future research.

Dynamic contrast-enhanced MRI

Angiogenesis in prostate cancer occurs because of vascular growth factors which are secreted in response to local hypoxia and lack of nutrients. Neoangiogenesis is pathologically seen as increased micro-vessel density (MVD) which correlates well with the Gleason score. It can be studied non-invasively and in a reproducible manner using dynamic contrast-enhanced MRI (DCE-MRI). DCE-MRI exploits the dynamic uptake and rapid washout of gadolinium chelate to show the typical pharmacokinetics of the cancerous tissue. A bolus of 0.1-0.2 mmol/kg low molecular weight (LMW) gadolinium chelate is administered intravenously at 2-4 ml/sec. Entire prostate is then imaged using a combination of fast and slow sequences. Fast sequences have a high temporal resolution (1-4 sec) and provide improved tissue characterization based on accurate quantification of different pharmacokinetic enhancement parameters.[56] Slow sequences have high spatial resolution and low temporal resolution (30 sec).[56]

Analysis may be done in qualitative, semi-quantitative, and quantitative manner. In quantitative analysis, the behavior of a volume of contrast in the intravascular versus interstitial space is estimated over a period of time. Using complex mathematical models, a few pharmacokinetic

quantitative parameters are calculated: V_e : volume of interstitial space; K_{ep} : exchange rate constant; K_{trans} : permeability or blood flow; and in Tofts model, $K_{ep} = K_{trans}/V_e$.[\[57\]](#) To a radiologist, the quantitative parameters are presented as colored parametric maps, overlaid over the conventional T2W images. Red areas represent high microvascular permeability with low extracellular-extravascular space (EES) fraction, typical of cancer. Blue areas represent areas of low permeability and high EES fraction, typical of normal tissue. Green areas are indeterminate areas. Tumor vessels generally have higher permeability than normal tissue.

Strength of DCE-MRI is its accuracy and high sensitivity of the order of 87-90%.[\[5859\]](#) Its drawbacks include limited discrimination of cancer from “prostatitis” in the PZ and “vascularized BPH nodules” in the TZ. Further, there is a lack of standardization in data acquisition protocols and shortage of commercially available tools for pharmacokinetic analysis. Current clinical use of DCE-MRI is for all indications of prostate cancer, viz., early detection, localization, characterization, staging, biopsy guidance, and active surveillance. However, its correlation with prognostic histopathologic markers of cancer angiogenesis has not been well studied and remains an area of future research.

Multi-parametric MRI

All functional MRI techniques have strengths and shortcomings, and can therefore be combined in multi-parametric MRI (MP MRI) to increase the accuracy of prostate cancer diagnosis. Minimal requirement for MP MRI is the combination of conventional T1W and T2W imaging with at least one functional MR technique, ideally using a combination of pelvic phased array and ERCs. No formal practice guidelines are currently available for the use of MP MRI. However, the proposed indications include more than one previously negative TRUS-guided random biopsy, pretreatment staging, active surveillance, and prior to focal ablative therapy.[\[51\]](#) High sensitivity of DCE-MRI may be used for the initial evaluation of potential tumor locations. Other functional techniques may then be subsequently added to increase specificity for cancer localization. Similarly, patients with previously negative systematic biopsy and persistently raised serum PSA may undergo MRS. Negative MRS saves a re-biopsy by excluding a high-grade tumor, supporting the choice for active surveillance. On the other hand, a positive MRS would suggest a re-biopsy, preferably targeted.[\[60\]](#) Computer programs (CAD) that allow display and evaluation of more than two different MP MRI images on one monitor are now being developed for the integrated interpretation of both anatomic and complex functional data to achieve reproducible results.[\[51\]](#)

MRI-Guided Prostate Biopsy

Standard TRUSgBx is random, prone to undersampling and suffers from inaccurate cancer detection and Gleason score grading. MRI-guided biopsy provides more accurate images, offering a possibility of more precise targeting. MRI guidance can assist to improve the diagnostic yield of prostate biopsy in three ways. In the first technique, and also the simplest, MRI is done separately. The location of suspected cancer so found helps the operator to draw a mental picture to specifically allow biopsy from those suspicious areas using standard TRUS guidance. Using this technique, an overall detection rate of 25% has been achieved, which is higher than 9% achieved by standard TRUSgBx without prior MRI.[61] In the second technique, the MRI datasets are co-registered with landmarks during TRUS, the so-called real-time virtual sonography. This is also referred to as the fusion, hybrid, or MRI-guided TRUS biopsy.[62] The experience with this technique is currently limited. Both these techniques retain the real-time capability of TRUS, the hybrid technique being more accurate. A recent report on the initial experience of real-time 2D TRUSgBx synchronized with MR imaging, displayed in parallel on the same screen (hybrid system), allowed a 61% increase in the cancer detection rate compared to systematic TRUS technique alone.[63] The third technique is a true MRI-guided biopsy using open or closed bore magnet.[64] Open magnets allow real-time patient access and image guidance, but typically possess lower resolution with field strengths of 0.3 T or 0.5 T. This is only possible with the use of MR-friendly equipment and compatible robotic/automatic guidance. These new techniques are currently under active research. Computer-aided real-time navigation allows needle placement with digital accuracy. This technological global positioning system like 3D imagery, has opened attractive opportunities for precise ablative therapies like high-intensity focused ultrasound (HIFU), interstitial brachytherapy, and modern endoscopic surgery, causing minimum adjacent tissue damage. Traditional side effects of surgery like impotence due to injury to neurovascular bundle and incontinence due to sphincter injury are therefore minimized.[65]

MRI-guided prostate biopsy is technically feasible and can be done routinely. It improves cancer detection and appears most promising. It is typically performed in patients with previously negative TRUSgBx. However, even when MRI-guided biopsy is planned, diagnostic MRI must be performed in a separate session because the image post-processing and exact tumor localization is time intensive. Limited availability, long procedure time, technically challenging MRI environment, long procedure time, limited access for manual instrument handling, and need for MRI-compatible equipment remain its limitations.

MRI before Prostate Biopsy

TRUSgBx is false negative in 20% cases of prostate cancer.[63] Those in whom it is detected, it underestimates the volume and grade of cancer. Also, the post biopsy MRI falsely overstages cancer in another 20% due to biopsy induced artifacts.[66] MRI is generally recommended 8 weeks after TRUSgBx. However, this delay in scheduling MRI appears unjustified as it increases patient anxiety and reduces biopsy-related artifacts in no more than half the patients. It is currently being debated whether or not to consider MRI before biopsy. Current clinical guidelines have underplayed the role of MRI, mainly owing to the poor-quality images from the low field strength magnets and the biopsy-induced artifacts on MRI. Further, the verification of low-risk, organ-confined disease by MRI is considered expensive and time consuming. However, the technological advances in prostate MRI in recent years demand re-evaluation of its status.[51] Therefore, a pre-biopsy MRI leads to more refined diagnostic pathway in selecting patients with significant disease who need treatment while excluding others. Further, the distinction between stage T2 and T3 disease by MRI is done better before biopsy.

Issue of Prostate Evasive Anterior Tumors

A significant number of anteriorly located cancers are diagnosed relatively late. These are missed by TRUSgBx as the biopsies tend to be laterally directed, focusing mainly at the PZ. These “hidden cancers” are located anterior to the urethra in the TZ (49%), anterior horns of PZ (36%), or both (8%). The prostate evasive anterior tumors (PEAT) are suspected when high or increasing PSA levels are present despite repeatedly negative biopsies. These patients are often kept under close clinical surveillance. MRI is now recommended to locate such cancers after adequate anterior and TZ biopsies have failed.[6768]

Problem of Repeat Biopsy

A repeat biopsy for clinically suspected prostate cancer poses a real challenge in those who report a consistently elevated PSA despite a negative biopsy. One way forward would be to increase the number of biopsy cores but with attendant increase in biopsy-related morbidity. Alternatively, the biopsy procedure could be made “targeted” to suspicious areas based on RTE/CEUS/MP MRI results. However, an attractive emerging technology may soon become available. Herein, the computer-aided registration of the needle location during real-time TRUS (or MRI or fusion) provides a precise spatial record of 3D location of every biopsy core.[69] This allows the operator

to perform the repeat biopsies only from the previously non-sampled areas. This biopsy technique is thought to be more precise than the external template-based guided approaches.

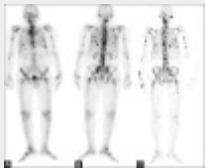
MRI using 3 T versus 1.5 T Systems and use of ERC in Prostate Cancer

All MR techniques, both anatomical and functional, specifically benefit from 3T magnets. The SNR increases linearly with increasing field strength. Gain in SNR at 3T can be utilized in several ways, one of which could be by simply reducing the acquisition time. The use of ERC increases the SNR and, therefore, staging accuracy, when used with 1.5 T system.[70] High-resolution MRI is possible without ERC on 3T magnet using pelvic phased-array coils.[71] However, concurrent use of ERC with 3T allows one to take full advantage of increased SNR. Also, there is improved resolution, both spatial and temporal. Both spatial and temporal resolution must be sufficiently high in DCE-MRI, which is a reality at 3T. Growing availability of 3T systems has now opened up new opportunities for clinical applications and research. However, the limitations of 3T are fourfold power deposition by RF pulses. This can be reduced by the use of low specific absorption rate (SAR) sequences. The 3T images are more prone to susceptibility-induced artifacts, especially when ERC is filled with air. It is particularly relevant with DWI which is more prone to both motion and susceptibility-induced distortion. ERC is expensive, causes patient discomfort, and is incompatible with intensity-modulated radiation therapy (IMRT) planning due to deformation of prostate and image fusion difficulties.[72]

Other Imaging Modalities

The role of a computed tomography (CT) scan is limited to pelvic lymph node evaluation and detection of distant metastasis in patients with known prostate cancer. Radionuclide ^{99}Tc bone scan [Figures 4A and B] is the standard technique employed to evaluate the presence of bone metastasis in those with high-risk disease (PSA >20 ng/ml). It is not indicated in low-risk disease having PSA <10 ng/ml. ProstaScint Scan (antibody scan) is currently undergoing intense investigations for imaging the tumor both in bones and soft tissues. It is sometimes used to assess if the recurrence is local or systemic. However, the nonspecific gastrointestinal uptake may be falsely interpreted as metastatic disease in this technique. The [18F]--fluorodeoxyglucose positron emission tomography/CT (^{18}F FDG PET/CT) has virtually no role in the evaluation of primary prostate cancer, especially if it is also low grade. It may be used for restaging a recurrent disease, nodal evaluation, or treatment response. Recently, choline PET has been specifically found to be useful in this respect. Fluoride-PET scan [Figure 4C], being a tomographic technique, has a much

higher sensitivity and resolution than the conventional radionuclide bone scan.



[View larger version](#)

Figure 4(A-C). A 76-year-old man presented with metastatic prostate carcinoma, and his serum PSA was 43.0 ng/ml. Radionuclide imaging included conventional ^{99m}Tc bone scan, both anterior (A) and posterior (B) views, and ^{18}F -PET/CT scan (C). Bone scan showed multiple foci of increased skeletal uptake of isotope suggesting disseminated metastases, involving skull, spine, ribs, pelvis, both humeri and femora. While the FDG-PET/CT (not shown) failed to detect these bony metastases, the ^{18}F -PET/CT performed significantly better than the bone scan by showing several additional foci of skeletal metastases

In summary, the prostate cancer imaging has witnessed remarkable advances in recent years, primarily in its early detection. TRUS with all its modifications, viz., CEUS, RTE, 3D TRUS, etc., have come a long way in improving the diagnostic yield, but is yet to find place in the current diagnostic algorithms. Targeted biopsies by modifications of TRUS (CEUS, RTE), 3D, and fusion with MRI have a potential to increase cancer detection rate and decrease unnecessary biopsy cores, making the procedure less invasive. However, the emerging MP MRI has largely eclipsed all other imaging advances relating to prostate cancer. Overwhelming evidence is available to support that MRI is all set to play an increasingly important role in all aspects of prostate cancer management including early detection, accurate biopsy, precise treatment, and reliable follow-up. This makes MRI almost a practical “one-stop shop” in improving the clinical outcomes. Recent recommendations based on the consensus meeting of the European Association of Urology (EAU) on the standard methods of conduct, interpretation, and reporting of MP MRI for prostate cancer detection and localization are available.[73] It is hoped that widespread incorporation of these recommendations will allow a more consistent and standardized approach to MRI, optimizing the diagnostic pathway. However, these would require validation in prospective trials before developing into protocols.

Acknowledgment

The author expresses his gratitude to Dr. Vishal Tambade, Dr. Chandan J Das, Dr. Durgesh Dwivedi and Dr. Rakesh Kumar for their valuable contribution.

Footnotes

Source of Support: Nil

Articles from The Indian Journal of Radiology & Imaging are provided here courtesy of Medknow Publications

PMC Copyright Notice

The articles available from the PMC site are protected by copyright, even though access is free. Copyright is held by the respective authors or publishers who provide these articles to PMC. Users of PMC are responsible for complying with the terms and conditions defined by the copyright holder.

Users should assume that standard copyright protection applies to articles in PMC, unless an article contains an explicit license statement that gives a user additional reuse or redistribution rights. PMC does not allow automated/bulk downloading of articles that have standard copyright protection.

See the copyright notice on the PMC site, <https://www.ncbi.nlm.nih.gov/pmc/about/copyright/>, for further details and specific exceptions.

References

1. Three Year Report of Population Based Cancer Registries (2009-2011). National Centre for Disease Informatics and Research. 2013 2. National Cancer Registry Progame, ICMR; p. 57
2. Siegel R, Ma J, Zou Z, Jemal A, authors. Cancer statistics, 2014. *CA Cancer J Clin.* 2014;64:9–29. [[PubMed](#)]
3. Okihara K, Shiraishi T, Ukimura O, Mizutani Y, Kawauchi A, Miki T, authors. Current trends in diagnostic and therapeutic principles for prostate cancer in Japan. *Int J Clin Oncol.* 2008;13:239–43. [[PubMed](#)]
4. Syrigos KN, Karapanagiotou E, Harrington KJ, authors. Prostate cancer in the elderly. *Anticancer Res.* 2005;25:4527–33. [[PubMed](#)]
5. Bostwick DG, Eble JN, authors. *Urological surgical pathology.* 2007. St. Louis: Mosby; p. 468
6. Epstein JI, Allsbrook WC Jr, Amin MB, Egevad LL, authors; ISUP grading committee. The 2005 International Society of Urologic Pathology (ISUP) Consensus Conference on Gleason grading of Prostatic Carcinoma. *Am J Surg Pathol.* 2005;29:1228–42. [[PubMed](#)]
7. Schröder FH, van der Maas P, Beemsterboer P, Kruger AB, Hoedemaeker R, Rietbergen J, et al., authors. Evaluation of the digital rectal examination as a screening test for prostate cancer. Rotterdam section of the European Randomized Study of Screening for Prostate Cancer. *J Natl Cancer Inst.* 1998;90:1817–23. [[PubMed](#)]
8. Gretzer MB, Partin AW, authors. PSA markers in prostate cancer detection. *Urol Clin North Am.* 2003;30:677–86. [[PubMed](#)]
9. Wilson SS, Crawford ED, authors. Screening for prostate cancer: Current recommendations. *Urol Clin North Am.* 2004;31:219–26. [[PubMed](#)]
10. Carter HB, Partin AW, authors; Retik AB, Vaughan ED Jr, Wein AJ, editors. *Diagnosis and staging of prostate cancer.* Campbell's Urology. 2002. 8th ed. Philadelphia, Pa: WB Saunders Co; p. 3055–79
11. Shteynshlyuger A, Andriole GL, authors. Prostate cancer: To screen or not to screen? *Urol Clin North Am.* 2010;37:1–9.

[\[PubMed\]](#)

12. Derweesh IH, Rabets JC, Patel A, Jones JS, Zippe C, authors. Prostate biopsy: Evolving indications and techniques. *Contemp Urol*. 2004;16:28–32
13. Djavan B, Remzi M, Marberger M, authors. When to biopsy and when to stop biopsying. *Urol Clin North Am*. 2003;30:253–62. [\[PubMed\]](#)
14. Schröder FH, Hugosson J, Roobol MJ, Tammela TL, Ciatto S, Nelen V, et al., authors. Screening and prostate-cancer mortality in a randomized European Study. *N Eng J Med*. 2009;360:1320–8
15. Chun FK, de la Taille A, van Poppel H, Marberger M, Stenzl A, Mulders PF, et al., authors. Prostate Cancer Gene 3 (PCA3): Development and Internal validation of a novel biopsy nomogram. *Eur Urol*. 2009;56:659–67. [\[PubMed\]](#)
16. Norberg M, Egevad L, Holmberg L, Sparén P, Norlén BJ, Busch C, authors. The sextant protocol for ultrasound-guided core biopsies of the prostate underestimates the presence of cancer. *Urology*. 1997;50:562–6. [\[PubMed\]](#)
17. Naughton CK, Smith DS, Humphrey PA, Catalona WJ, Keetch DW, authors. Clinical and pathologic tumor characteristics of prostate cancer as a function of the number of biopsy cores: A retrospective study. *Urology*. 1998;52:808–13. [\[PubMed\]](#)
18. Patel AR, Jones JS, Rabets J, DeOreo G, Zippe CD, authors. Para-sagittal biopsies add minimal information in repeat saturation prostatic biopsy. *Urology*. 2004;63:87–9. [\[PubMed\]](#)
19. Djavan B, Ravery V, Zlotta A, Dobronski P, Dobrovits M, Fakhari M, et al., authors. Prospective evaluation of prostate cancer detected on biopsies 1, 2, 3 and 4: When should we stop? *J Urol*. 2001;166:1679–83. [\[PubMed\]](#)
20. Noguchi M, Stamey TA, McNeal JE, Yemoto CM, authors. Relationship between systematic biopsies and histological features of 222 radical prostatectomy specimens: Lack of prediction of tumor significance for men with non palpable prostate cancer. *J Urol*. 2001;166:104–9. [\[PubMed\]](#)
21. Taneja SS, author. Imaging in the Diagnosis and Management of Prostate Cancer. *Rev Urol*. 2004;6:101–13. [\[PubMed\]](#)
22. Persti JC Jr, Chang JJ, Bhargava V, Shinohara K, authors. The optimal systematic prostate biopsy scheme should include 8 rather than 6 biopsies: Results of a prospective clinical trial. *J Urol*. 2000;163:163–6. [\[PubMed\]](#)
23. Babaian RJ, Toi A, Kamoi K, Troncoso P, Sweet J, Evans R, et al., authors. A comparative analysis of sextant and an extended 11-core multisite directed biopsy strategy. *J Urol*. 2000;163:152–7. [\[PubMed\]](#)
24. Heidenreich A, Bellmunt J, Bolla M, Joniau S, Mason M, Matveev V, et al., authors. EAU guidelines on prostate cancer. Part 1: Screening, diagnosis, and treatment of clinically localised disease. *Eur Urol*. 2011;59:61–71. [\[PubMed\]](#)
25. Srinivas V, Mehta H, Amin A, Choudhary R, Gadgil N, Ravishanker D, et al., authors. Carcinoma of the prostate- stage at initial presentation. *Int Urol Nephrol*. 1995;27:419–22. [\[PubMed\]](#)
26. Gupta NP, Ansari MS, Das SC, authors. Transrectal ultrasound guided biopsy for detecting early prostate cancer: An Indian experience. *Indian J Cancer*. 2005;42:151–4. [\[PubMed\]](#)
27. Ismail M, Peterson RO, Alexander AA, Newschaffer C, Gomella LG, authors. Colour Doppler imaging in predicting the biologic behavior of prostate cancer: Correlation with disease-free survival. *Urology*. 1997;50:906–12. [\[PubMed\]](#)
28. Kirby RS, author. Pre-treatment staging of prostate cancer: Recent advances and future prospects. *Prostate Cancer Prostatic Dis*. 1997;1:2–10. [\[PubMed\]](#)
29. Taverna G, Morandi G, Seveso M, Giusti G, Benetti A, Colombo P, et al., authors. Colour Doppler and microbubble contrast agent ultrasonography do not improve cancer detection rate in Transrectal systemic prostate biopsy sampling. *BJU Int*. 2011;108:1723–7. [\[PubMed\]](#)
30. Halpern EJ, Frauscher F, Strup SE, Nazarian LN, O’Kane P, Gomella LG, authors. Prostate: High-frequency Doppler US Imaging for cancer detection. *Radiology*. 2002;225:71–7. [\[PubMed\]](#)

31. Halpern EJ, Ramey JR, Strup SE, Frauscher F, McCue P, Gomella LG, authors. Detection of prostate cancer with contrast enhanced sonography using intermittent harmonic imaging. *Cancer*. 2005;104:2373–83. [[PubMed](#)]
32. Mitterberger M, Aigner F, Pinggera GM, Steiner E, Rehder P, Ulmer H, et al., authors. Contrast-enhanced colour doppler-targeted prostate biopsy: Correlation of a subjective blood-flow rating scale with the histopathological outcome of the biopsy. *BJU Int*. 2010;106:1315–8. [[PubMed](#)]
33. Brock M, von Bodman C, Sommerer F, Loppenberg B, Klien T, Deix T, et al., authors. Comparison of real-time elastography with gray-scale Ultrasonography for detection of organ-confined prostate cancer and extra capsular extension: A prospective analysis using whole mount sections after radical prostatectomy. *BJU Int*. 2011;108:E217–22. [[PubMed](#)]
34. Bloch BN, Rofsky NM, Baroni RH, Marquis RP, Pedrosa I, Lenkinski RE, authors. 3 Tesla magnetic resonance imaging of the prostate with combined pelvic phased-array and endorectal coils; Initial experience (1). *Acad Radiol*. 2004;11:863–7. [[PubMed](#)]
35. Narayanan R, Werahera PN, Barqawi A, Crawford ED, Shinohara K, Simoneau AR, et al., authors. Adaptation of a 3D prostate cancer atlas for transrectal ultrasound guided target-specific biopsy. *Phys Med Biol*. 2008;53:N397–406. [[PubMed](#)]
36. Stamey TA, Donaldson AN, Yemoto CE, McNeal JE, Sözen S, Gill H, authors. Histological and clinical findings in 896 consecutive prostates treated only with radical retropubic prostatectomy: Epidemiologic significance of annual changes. *J Urol*. 1998;160:2412–7. [[PubMed](#)]
37. Augustin H, Hammerer PG, Blonski J, Graefen M, Palisaar J, Daghofer F, et al., authors. Zonal location of prostate cancer: Significance for disease-free survival after radical prostatectomy? *Urology*. 2003;62:79–85. [[PubMed](#)]
38. Puech P, Betrouni N, Makni N, Dewalle AS, Villers A, Lemaitre L, authors. Computer-assisted diagnosis of prostate cancer using DCE-MRI data: Design, implementation and preliminary results. *Int J Comput Assist Radiol Surg*. 2009;4:1–10. [[PubMed](#)]
39. Katahira K, Takahara T, Kwee TC, Oda S, Suzuki Y, Morishita S, et al., authors. Ultra-high-b-value diffusion-weighted MR imaging for the detection of prostate cancer: Evaluation in 201 cases with histopathological correlation. *Eur Radiol*. 2011;21:188–96. [[PubMed](#)]
40. Tamada T, Sone T, Jo Y, Toshimitsu S, Yamashita T, Yamamoto A, et al., authors. Apparent diffusion coefficient values in peripheral and transition zones of the prostate: Comparison between normal and malignant prostatic tissues and correlation with histologic grade. *J Magn Reson Imaging*. 2008;28:720–6. [[PubMed](#)]
41. Tanimoto A, Nakashima J, Kohno H, Shinmoto H, Kuribayashi S, authors. Prostate cancer screening: The clinical value of diffusion-weighted imaging and dynamic MR imaging in combination with T2-weighted imaging. *J Magn Reson Imaging*. 2007;25:146–52. [[PubMed](#)]
42. Ren J, Huan Y, Wang H, Zhao H, Ge Y, Chang Y, et al., authors. Diffusion-weighted imaging in normal prostate and differential diagnosis of prostate diseases. *Abdom Imaging*. 2008;33:724–8. [[PubMed](#)]
43. Mazaheri Y, Shukla-Dave A, Hricak H, Fine SW, Zhang J, Inurrigarro G, et al., authors. Prostate cancer: Identification with combined diffusion-weighted MR imaging and 3D 1H MR spectroscopic imaging-correlation with pathologic findings. *Radiology*. 2008;246:480–8. [[PubMed](#)]
44. Reinsberg SA, Payne GS, Riches SF, Ashley S, Brewster JM, Morgan VA, et al., authors. Combined use of diffusion-weighted MRI and 1H MR spectroscopy to increase accuracy in prostate cancer detection. *AJR Am J Roentgenol*. 2007;188:91–8. [[PubMed](#)]
45. Kingsley PB, Monahan WG, authors. Selection of optimum b factor for diffusion weighted magnetic resonance imaging assessment of ischemic stroke. *Magn Reson Med*. 2004;51:996–1001. [[PubMed](#)]

46. Pickles MD, Gibbs P, Sreenivas M, Turnbull LW, authors. Diffusion-weighted imaging of normal and malignant prostatic tissue at 3.0T. *J Magn Reson Imaging*. 2006;23:130–4. [[PubMed](#)]
47. Hambrock T, Somford DM, Huisman HJ, van Oort IM, Witjes JA, Hulsbergen-van de Kaa CA, et al., authors. Relationship between apparent diffusion coefficients at 3.0-T MR imaging and Gleason grade in peripheral zone prostate cancer. *Radiology*. 2011;259:453–61. [[PubMed](#)]
48. Kim JH, Kim JK, Park BW, Kim N, Cho KS, authors. Apparent diffusion coefficient: Prostate cancer versus noncancerous tissue according to anatomical region. *J Magn Reson Imaging*. 2008;28:1173–9. [[PubMed](#)]
49. Blackledge MD, Leach MO, Collins DJ, Koh DM, authors. Computed diffusion weighted MR imaging may improve tumor detection. *Radiology*. 2011;261:573–81. [[PubMed](#)]
50. Rosenkrantz AB, Mannelli L, Kong X, Niver BE, Berkman DS, Babb JS, et al., authors. Prostate cancer: Utility of fusion of T2-weighted and high b-value diffusion-weighted images for peripheral zone tumor detection and localization. *J Magn Reson Imaging*. 2011;34:95–100. [[PubMed](#)]
51. Hoeks CM, Barentsz JO, Hambrock T, Yakar D, Somford DM, Heijmink SW, et al., authors. Prostate cancer: MULTIPARAMETRIC MR imaging for detection, localization, and staging. *Radiology*. 2011;261:46–66. [[PubMed](#)]
52. Kurhanewicz J, Vigneron DB, Hricak H, Narayan P, Carroll P, Nelson SJ, authors. Three-dimensional H-1 MR spectroscopic imaging of the in situ human prostate with high (0.24-0.7-cm³) spatial resolution. *Radiology*. 1996;198:795–805. [[PubMed](#)]
53. Choi YJ, Kim JK, Kim N, Kim KW, Choi EK, Cho KS, authors. Functional MR Imaging of prostate cancer. *Radiographics*. 2007;27:63–75. [[PubMed](#)]
54. Zakian KL, Sircar K, Hricak H, Chen HN, Shukla- Dave A, Eberhardt S, et al., authors. Correlation of proton MR spectroscopic imaging with Gleason score based on step-section pathologic analysis after radical prostatectomy. *Radiology*. 2005;234:804–14. [[PubMed](#)]
55. Yu KK, Scheidler J, Hricak H, Vigneron DB, Zaloudek CJ, Males RG, et al., authors. Prostate cancer: Prediction of extracapsular extension with endorectal MR imaging and three-dimensional proton MR spectroscopic imaging. *Radiology*. 1999;213:481–8. [[PubMed](#)]
56. Verma S, Turkbey B, Muradyan N, Rajesh A, Cornud F, Haider MA, et al., authors. Overview of dynamic contrast-enhanced MRI in prostate cancer diagnosis and management. *AJR Am J Roentgenol*. 2012;198:1277–88. [[PubMed](#)]
57. Tofts PS, author. Modeling tracer kinetics in dynamic Gd-DTPA MR imaging. *J Magn Reson Imaging*. 1997;7:91–101. [[PubMed](#)]
58. Sung YS, Kwon HJ, Park BW, Cho G, Lee CK, Cho KS, et al., authors. Prostate cancer detection on dynamic contrast-enhanced MRI: Computer-aided diagnosis versus single perfusion parameter maps. *AJR Am J Roentgenol*. 2011;197:1122–9. [[PubMed](#)]
59. Fütterer JJ, Heijmink SW, Scheenen TW, Veltman J, Huisman HJ, Vos P, et al., authors. Prostate cancer localization with dynamic contrast-enhanced MR imaging and proton MR spectroscopic imaging. *Radiology*. 2006;241:449–58. [[PubMed](#)]
60. De Visschere P, Oosterlinck W, De Meerleer G, Villeirs G, authors. Clinical and Imaging tools in the early diagnosis of prostate cancer, A review. *JBR-BTR*. 2010;93:62–70. [[PubMed](#)]
61. Kumar V, Jagannathan NR, Kumar R, Thulkar S, Gupta SD, Hemal AK, et al., authors. Transrectal ultrasound-guided biopsy of prostate voxels identified as suspicious of malignancy on three-dimensional (1) H MR spectroscopic imaging in patients with abnormal digital rectal examination or raised prostate specific antigen level of 4-10 ng/ml. *NMR Biomed*. 2007;20:11–20. [[PubMed](#)]
62. Kaplan I, Oldenberg NE, Meskell P, Blake M, Church P, Holupka EJ, authors. Real time MRI-ultrasound image guided stereotactic prostate biopsy. *Magn Reson Imaging*. 2002;20:295–9. [[PubMed](#)]

63. Hirahara N, Ukimora O, Fujihara A, authors. Video: Hybrid real time ultrasound system fused with virtual 3D CT/MRI for image guided surgery. *J Urol*. 2010;183(suppl):185
64. Lattouf JB, Grubb RL 3rd, Lee SJ, Bjurlin MA, Albert P, Singh AK, et al., authors. Magnetic resonance imaging-directed transrectal ultrasonography-guided biopsies in patients at risk of prostate cancer. *BJU Int*. 2007;99:1041–6. [[PubMed](#)]
65. Atalar E, Menard C, authors. MR-Guided interventions for prostate cancer. *Magn Reson Imaging Clin N Am*. 2005;13:491–504. [[PubMed](#)]
66. White S, Hricak H, Forstner R, Kurhanewicz J, Vigneron DB, Zaloudek CJ, et al., authors. Prostate cancer: Effect of post biopsy hemorrhage on interpretation of MR images. *Radiology*. 1995;195:385–90. [[PubMed](#)]
67. Lawrentschuk N, Haider MA, Daljeet N, Evans A, Toi A, Finelli A, et al., authors. ‘Prostatic evasive anterior tumours’: The role of magnetic resonance imaging. *BJU Int*. 2010;105:1231–6. [[PubMed](#)]
68. McNeal JE, Redwine EA, Friehe FS, Stamey TA, authors. Zonal distribution of prostatic adenocarcinoma: Correlation with histologic pattern and direction of spread. *Am J Surg Pathol*. 1988;12:897–906. [[PubMed](#)]
69. Mozer P, Baumann M, Daanen V, Bordenave M, Thibault F, Conort P, et al., authors. Free hand 3D-TRUS prostate biopsies mapping. *J Urol*. 2010;183(Suppl):833
70. Fütterer JJ, Engelbrecht MR, Jager GJ, Hartman RP, King BF, Hulsbergen-Van de Kaa CA, et al., authors. Prostate cancer: Comparison of local staging accuracy of pelvic phased-array coil alone versus integrated endorectal-pelvic phased-array coils. Local staging accuracy of prostate cancer using endorectal coil MR imaging. *Eur Radiol*. 2007;17:1055–65. [[PubMed](#)]
71. Girouin N, Mège-Lechevallier F, Tonina Senes A, Bissery A, Rabilloud M, Maréchal JM, et al., authors. Prostate dynamic contrast-enhanced MRI with simple visual diagnostic criteria: Is it reasonable? *Eur Radiol*. 2007;17:1498–509. [[PubMed](#)]
72. Villeirs GM, L Verstraete K, De Neve WJ, De Meerleer GO, authors. Magnetic resonance imaging anatomy of the prostate and periprostatic area: A guide for radiotherapists. *Radiother Oncol*. 2005;76:99–106. [[PubMed](#)]
73. Dickinson L, Ahmed HU, Allen C, Barentsz JO, Carey B, Fütterer JJ, et al., authors. Magnetic Resonance Imaging for the Detection, localization, and characterization of prostate cancer: Recommendations from a European consensus meeting. *Eur Urol*. 2011;59:477–94. [[PubMed](#)]

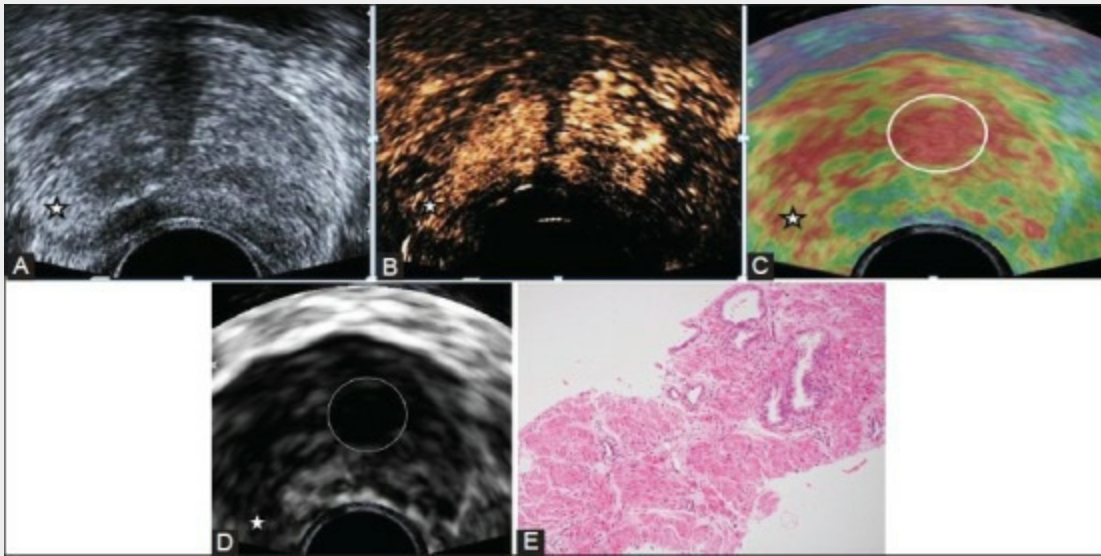


Figure 1(A-E).

A 76-year-old man with lower urinary tract symptoms, serum PSA 32.2 ng/ml. Gray scale TRUS (A), CEUS images (B), paired elastogram (colour C; gray scale D), and photomicrograph (E) (H and E) of TRUS guided biopsy; all showing an ill circumscribed nodule (star) in the PZ of mid-gland on the right corresponding to an area of abnormality on per-rectal examination. This nodule is hyperechoic (A), shows enhancement (B) and relatively hard (C, D). Hard areas are displayed as red and soft areas as green. On histopathology the nodule was diagnosed to be a cancer on histopathology. Three out of 12 cores showed features of high grade, Gleason score 10 (5+5), adenocarcinoma. Note the persistent enhancement of the central gland and another larger hard nodule (C, D; encircled) in the central gland on the left. This was a benign hyperplastic nodule on histopathology.

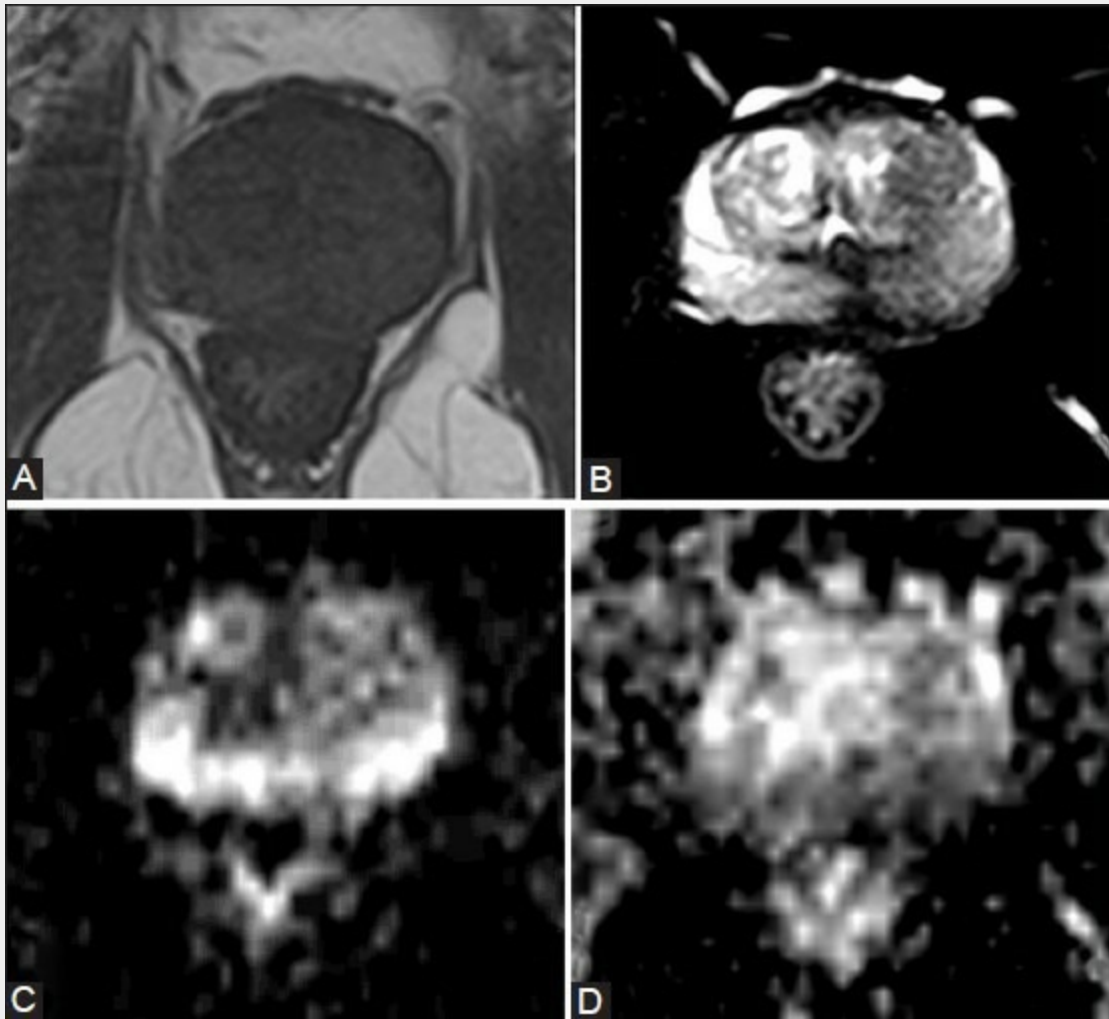


Figure 2(A-D).

A 77-year-old man reported with serum PSA 11.6 ng/ml. MR images at the mid-gland, T1WI (A), T2WI (B), DWI (C), and ADC map (D). The intermediate signal intensity gland is seen on T1WI; T2WI shows ill-defined hypointense area posteriorly at the PZ, especially prominent on the left. There is no extracapsular extension or regional adenopathy. The entire PZ on the DWI shows restricted diffusion as evidenced by bright signal on DWI and dark signal on ADC maps. On TRUS-guided biopsy, 4 out of 12 cores showed features of adenocarcinoma, Gleason score 9 (4 + 5)

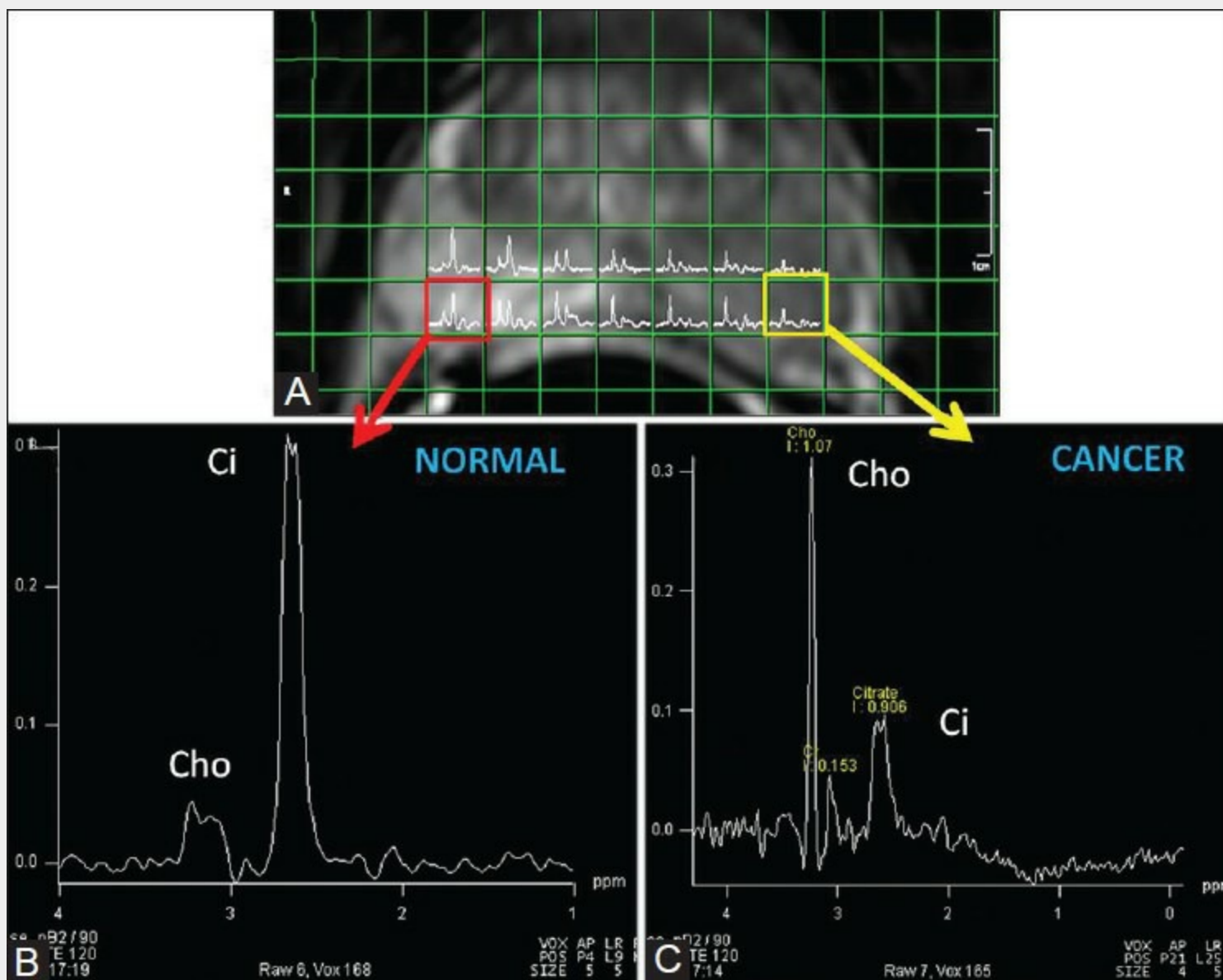


Figure 3(A-C).

A 69-year-old man presented with serum PSA 21.4 ng/ml. Overlay of MR spectroscopic matrix and multi-voxel spectra on the T2W image of mid-prostate (A). The voxel on the left (yellow) shows markedly reduced citrate (Ci) signal and increased chol-creatine (Cho + Cr)-to-citrate ratio consistent with cancer (C). On TRUS-guided biopsy, this was later confirmed to be a high-grade cancer, Gleason score 9 (5 + 4). The voxel on the right (red) represents a normal spectrum (B). The addition of spectroscopy to MRI improves the ability to localize the cancer more precisely reducing the inter-observer variability. Higher the metabolite ratio, higher are the chances of finding a high-grade cancer

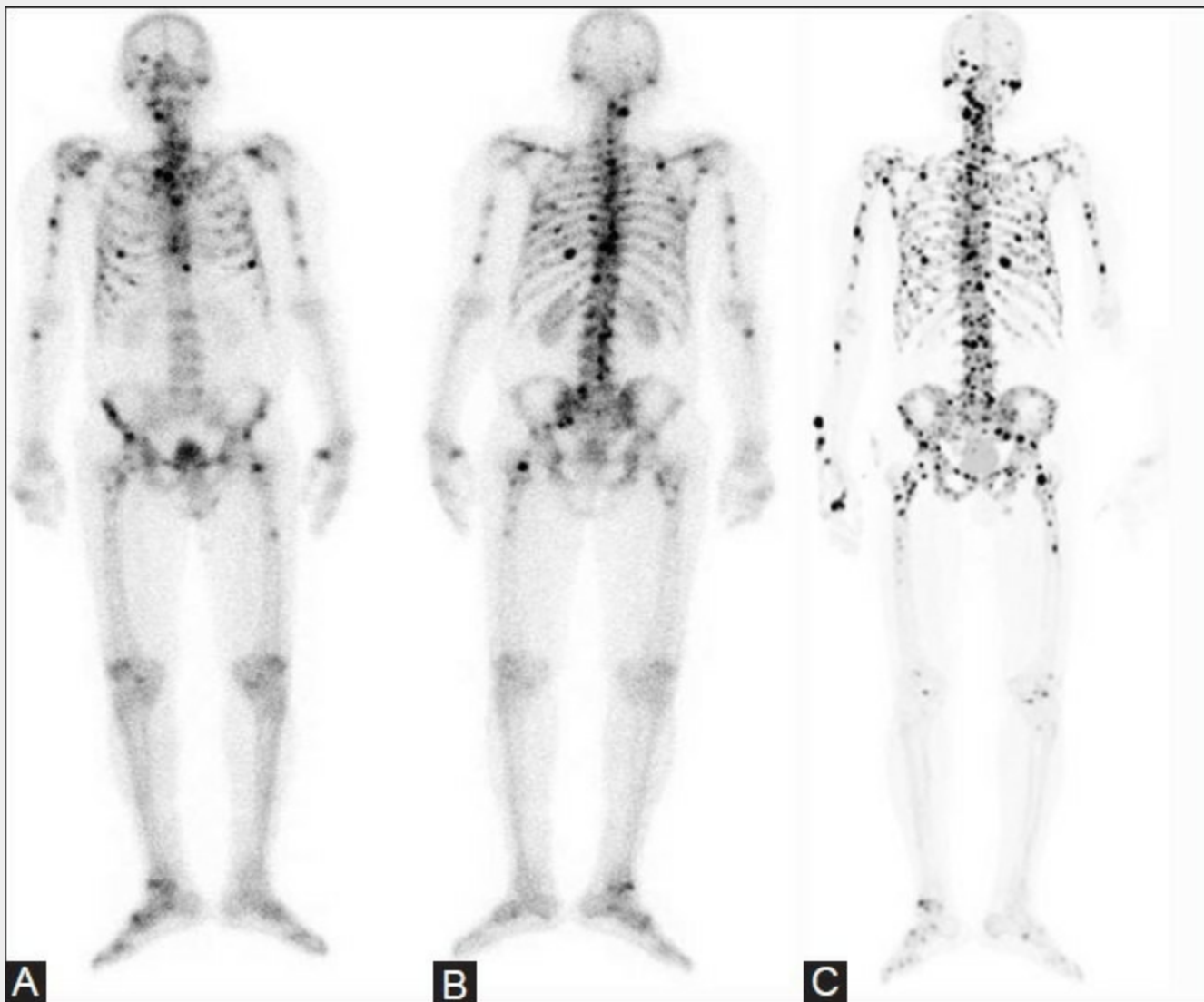


Figure 4(A-C).

A 76-year-old man presented with metastatic prostate carcinoma, and his serum PSA was 43.0 ng/ml. Radionuclide imaging included conventional ^{99m}Tc bone scan, both anterior (A) and posterior (B) views, and ^{18}F -PET/CT scan (C). Bone scan showed multiple foci of increased skeletal uptake of isotope suggesting disseminated metastases, involving skull, spine, ribs, pelvis, both humeri and femora. While the FDG-PET/CT (not shown) failed to detect these bony metastases, the ^{18}F -PET/CT performed significantly better than the bone scan by showing several additional foci of skeletal metastases